

# Inducing a superconducting-to-normal-state first-order phase transition in overdoped $\text{Bi}_2\text{Sr}_2\text{Ca}_{0.92}\text{Y}_{0.08}\text{Cu}_2\text{O}_{8+\delta}$ by ultrashort laser pulses

G. Coslovich,<sup>1,2</sup> C. Giannetti,<sup>3</sup> F. Cilento,<sup>1,2</sup> S. Dal Conte,<sup>4</sup> G. Ferrini,<sup>3</sup> P. Galinetto,<sup>4</sup> M. Greven,<sup>5,6</sup> H. Eisaki,<sup>7</sup> M. Raichle,<sup>8</sup> R. Liang,<sup>8</sup> A. Damascelli,<sup>8</sup> and F. Parmigiani<sup>1,9</sup>

<sup>1</sup>*Department of Physics, Università degli Studi di Trieste, Trieste I-34127, Italy*

<sup>2</sup>*Laboratorio Nazionale TASC, AREA Science Park, Basovizza Trieste I-34012, Italy*

<sup>3</sup>*Department of Physics, Università Cattolica del Sacro Cuore, Brescia I-25121, Italy*

<sup>4</sup>*Department of Physics A. Volta, Università degli Studi di Pavia, Pavia I-27100, Italy*

<sup>5</sup>*School of Physics and Astronomy, University of Minnesota, Minneapolis, Minnesota 55455, USA*

<sup>6</sup>*Department of Applied Physics, Stanford University, Stanford, California 94305, USA*

<sup>7</sup>*Nanoelectronics Research Institute, National Institute of Advanced*

*Industrial Science and Technology, Tsukuba, Ibaraki 305-8568, Japan*

<sup>8</sup>*Department of Physics & Astronomy, University of British Columbia, Vancouver, British Columbia V6T 1Z1, Canada*

<sup>9</sup>*Sincrotrone Trieste S.C.p.A., Basovizza I-34012, Italy*

(Dated: February 6, 2019)

We report on pump-probe reflectivity experiments on an overdoped  $\text{Bi}_2\text{Sr}_2\text{Ca}_{1-x}\text{Y}_x\text{Cu}_2\text{O}_{8+\delta}$  single crystal ( $T_C=78$  K), where a Fermi-liquid like normal phase is expected. The data show that the non-equilibrium superconducting gap linearly decreases with the photoinjected excitation density and that the superconducting phase instability is achieved when the non-equilibrium gap reaches 50% of the equilibrium value. These results constitute evidence for a first-order photoinduced superconducting-to-normal-state phase transition above a critical pump fluence.

PACS numbers: 74.40.Gh, 78.47.J-, 78.47.jg, 74.72.-h

## I. INTRODUCTION

The possibility of inducing an electronic first-order phase transition in high-temperature superconductors (HTSC), by means of ultra-short laser pulses, opens an important new route for studying these materials. In this scenario, the homogeneous superconducting phase becomes unstable as its free energy increases during the pulse duration<sup>1-3</sup>. Under such non-equilibrium conditions, the superconducting order parameter can coexist with the pseudogap or normal phase. For many years the exploration of the physics of this process has been a difficult task because of experimental limitations, mainly arising from laser induced heating of the samples<sup>4-7</sup>. Only recent all-optical pump-probe experiments on underdoped and optimally doped HTSC<sup>3,8,9</sup> have achieved control of the impulsive vaporization of the superconducting condensate in the high-intensity regime. This phenomenon has been observed as the saturation of the transient reflectivity variation ( $\Delta R/R$ ) signal associated with the superconducting phase<sup>3,8</sup>, in contrast to its linear fluence dependence in the low intensity regime<sup>6,10-14</sup>.

Nonetheless, the origin of this sub-linear response in the high-excitation regime remains unclear. So far its identification as a non-thermal electronic first-order phase transition<sup>1,2</sup> has been speculative, based on a comparison of the experimental fluence threshold to a simple BCS-model prediction<sup>3</sup>. A clear picture of the photoinduced non-equilibrium state is still lacking due to intrinsic difficulties to disentangle pseudogap and normal-phase signals in optimally and underdoped samples<sup>3,9</sup>, the fingerprint of the pseudogap phase being the  $\Delta R/R$  sign change between  $T^*$  and  $T_C$  observed in pump-probe

experiments when probing at 800 nm wavelength<sup>15</sup>.

Here we report the study of the high excitation regime of an overdoped sample, where we expect a Fermi-liquid-like underlying normal phase<sup>16</sup> and no  $\Delta R/R$  sign change between  $T^*$  and  $T_C$ , at variance with optimally and underdoped samples<sup>17</sup>, as we will show in this work. In particular we performed pump-probe optical reflectivity measurements at 800 nm on a  $\text{Bi}_2\text{Sr}_2\text{Ca}_{0.92}\text{Y}_{0.08}\text{Cu}_2\text{O}_{8+\delta}$  (Y-Bi2212) single crystal ( $T_C=78$  K). We report the instability of the superconducting state when the non-equilibrium gap has reached  $\approx 50\%$  of its equilibrium value. This is evidence of a first-order superconducting-to-normal-state phase transition induced by the 800 nm ultrashort pump laser pulse, in striking contrast to a thermally-induced 2<sup>nd</sup> order superconducting-to-normal-state transition, where the superconducting order parameter gradually decreases with temperature and vanishes at  $T_C$ .

The present work represents a landmark for the growing field of pump-probe techniques, which have been recently extended to the use of several probes, such as Raman scattering<sup>18</sup>, electron-diffraction<sup>19</sup>, angle-resolved photo emission<sup>20</sup> and broadband optical spectroscopy<sup>21</sup>. All these techniques require an intense ultra-short pump laser pulse, ranging from  $\sim 100 \mu\text{J}/\text{cm}^2$  in Ref. 20 to several  $\text{mJ}/\text{cm}^2$  in Ref. 19, to have reliable results. Our results finally clarify the effect of a pump laser pulse at high fluence on the superconducting condensate of HTSC.

In Sec. II we briefly report the experimental procedure. In Sec. III A we study the temperature dependence of the signal related to the superconducting phase in the low-excitation regime and we show that the decay rate is proportional to the superconducting order parameter  $\Delta$ . In

particular, we focus on the decay time divergence in the vicinity of  $T_C$ , where  $\Delta \rightarrow 0$  and thus a vanishing relaxation rate is measured<sup>10,11,13,22</sup>. In Sec. IIIB we discuss the dynamics as a function of fluence at a fixed temperature (10 K) well below  $T_C$ . Above a threshold pump fluence, the reflectivity variation deviates from the linear dependence and exhibits a saturation in agreement with previous experiments<sup>3,8,9</sup>. This discontinuity is identified with the condensate vaporization in the whole probed volume<sup>8</sup>. We then report the most important finding of this manuscript, i.e., the absence of a decay time divergence at this threshold point. A non-vanishing relaxation rate implies a finite superconducting gap value on the timescale involved in our experiment (picoseconds). We observe a linear decrease of the non-equilibrium gap with pump fluence before the photoinduced phase transition takes place.

## II. EXPERIMENTAL METHODS

Pump-probe measurements have been performed on an over-doped  $\text{Bi}_2\text{Sr}_2\text{Ca}_{0.92}\text{Y}_{0.08}\text{Cu}_2\text{O}_{8+\delta}$  ( $x=0.08$ ) single crystal with  $T_C=78 \text{ K} \pm 5 \text{ K}$ . The Y-substituted Bi2212 single crystal was grown in an image furnace by the traveling-solvent floating-zone technique with a non-zero Y content in order to maximize  $T_C$ <sup>23</sup>. The crystal was annealed in a flowing  $\text{O}_2:\text{N}_2$  mixture in order to increase the hole concentration and reach the overdoped side of the phase diagram. The sample was subsequently homogenized by further annealing in a sealed quartz ampoule, together with ceramic at the same oxygen content. In our experiments the 800 nm, 120 fs laser pulses were generated by a cavity dumped Ti:Sapphire oscillator. The use of a tunable repetition rate laser source allows us to avoid the experimental problem of average heating effects<sup>24</sup>. These effects prevented earlier observation of the photoinduced condensate vaporization<sup>6,7</sup>. In the time-resolved experiment the transient reflectivity variation is measured and we denote it as  $\Delta R/R$ .

## III. RESULTS AND DISCUSSION

### A. Low-fluence results as a function of temperature

In the low-intensity regime several common trends have been recognized based on the large amount of experimental data reported on HTSC, such as, i) the appearance below  $T_C$  of a  $\Delta R/R$  signal proportional to the photoexcited quasi-particle (QP) density<sup>3-14,22</sup>, ii) an intensity and temperature dependent decay time of this superconducting component<sup>5,6,9-14,22</sup> iii) the equivalence of the decay time observed probing at 800 nm and the gap dynamics observed in the THz spectral region<sup>14</sup>.

In Fig. 1 we plot the raw ( $\Delta R/R$ ) data of consecutive series of scans taken from 87 K down to 38 K at low pump fluence ( $\sim 4 \mu\text{J}/\text{cm}^2$ ). The positive signal

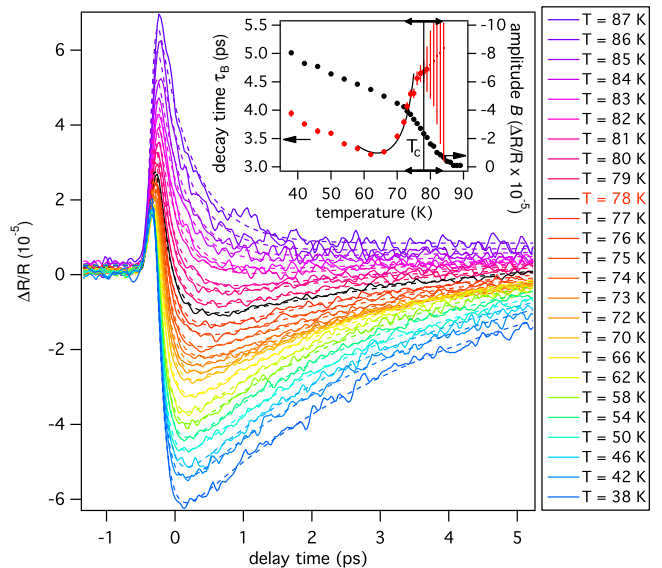


FIG. 1:  $\Delta R/R$  signal (solid lines) as a function of delay time at different temperatures (from 87 K to 38 K) on Y-Bi2212 overdoped single crystal ( $T_C=78 \text{ K}$ ). The fits to the experimental curves are the dashed lines (see the fitting function in the text). The negative component appearing just above  $T_C$  is the superconducting signal (SCS). The black line represents the  $\Delta R/R$  trace at  $T_C$ . In the inset we report the fit parameters of the SCS, i.e., the decay time,  $\tau_B$  (red circles), and amplitude,  $B$  (black circles). The error bars obtained from the fit procedure are displayed for all the data. The high uncertainty on the decay time above  $T_C$  led us to plot just the error bar and not the data point. The black arrow on the temperature axis of the inset shows the superconducting transition amplitude of the sample.

above  $T_C$  can be reproduced by a single exponential decay function,  $Ae^{-t/\tau_A}$ , convoluted with the time shape of the laser pulse, describing the relaxation of hot electrons via electron-phonon interaction<sup>25-27</sup> with a relaxation time  $\tau_A$  of about 440 fs. All the traces from room temperature down to 87 K did not show any substantial difference from the 87 K trace. In agreement with the literature<sup>17</sup>, no  $\Delta R/R$  sign change associated with the pseudogap phase is observed when probing at 800 nm wavelength on the overdoped sample, at variance with optimally and underdoped samples<sup>15</sup>.

The positive and fast signal survives also below  $T_C$ , superimposed to a negative signal that we recognize as the superconducting signal (SCS) proportional to the photoexcited QP density and that we capture with a single exponential function. The sum of these two functions,  $Ae^{-t/\tau_A} + Be^{-t/\tau_B}$ , is sufficient to reproduce all the experimental curves as shown in Fig. 1, where the dashed lines are the fits to the data. The relevant fit parameters of the SCS, i.e., the amplitude  $B$  and the decay time  $\tau_B$ , are plotted in the inset.

The decay time of the SCS,  $\tau_B$ , is shown, as a function of temperature, in the inset of Fig.1 (red circles).

Starting from 38 K the decay time decreases with temperature, reaching a minimum at 62 K of 3.3 ps. Above this temperature it rapidly increases reaching the value of 4.7 ps at  $T_C$ . At this temperature the order parameter vanishes ( $\Delta \rightarrow 0$ ), the SCS amplitude,  $B$ , is much smaller than  $A$  (the normal-state signal), and the uncertainty on the determination of its decay time strongly increases.

The increase in the decay time in the vicinity of  $T_C$  is in agreement with previous observations for other HTSC in the low-fluence regime<sup>10,11,13,22</sup> and it has been interpreted as the manifestation of a  $\propto 1/\Delta$  divergence predicted by several theoretical calculations for BCS superconductors<sup>10,28,29</sup>. Experimentally this divergence is smeared out because of the finite superconducting transition amplitude. However, from the analysis of the SCS decay time increase just below  $T_C$ , we can extract quantitative information about the superconducting gap.

A very useful model to interpret the non-equilibrium dynamics of superconductors in the low-intensity regime is the Rothwarf-Taylor model (RT)<sup>13,30,31</sup>. In this model, two QPs recombine to form a Cooper pair emitting a boson with energy larger than  $2\Delta$ . Since the reverse process has the same probability, the QP and the boson populations are in quasi-equilibrium and the actual relaxation is determined by inelastic processes. Within this model, one can write down a set of coupled rate equations, which have analytic solutions in two very important limiting cases, the weak and the strong bottleneck regimes<sup>13,30</sup>. In the first case, the boson inelastic decay rate is fast and the relaxation dynamics is equivalent to simple bimolecular dynamics<sup>12,14</sup>. In the second regime, namely the strong bottleneck one, the inelastic decay of the boson population strongly slows down the relaxation process. For a given superconductor, the dynamical regime is determined by the particular type of bosons considered in this dynamics. However, in both regimes and far enough from the critical temperature<sup>32</sup>, a very simple formula for the QP decay rate  $\gamma$  is valid

$$\gamma(T, \Delta(n_{ph}), n_{ph}) = (n_{ph} + n_T)\Gamma(T, \Delta(n_{ph})) \quad (1)$$

where  $n_T$  are the thermal QPs,  $n_{ph}$  are the photo-injected ones and  $\Gamma(T, \Delta)$  is a function of the microscopic probabilities for the scattering events involving QPs and bosons<sup>13</sup>. Given the QP population densities,  $n_{ph}$  and  $n_T$ , one can extract from the experimental QP decay rate  $\gamma$  the  $\Gamma(T, \Delta)$  function in the low-excitation limit. We stress that the use of this formula does not imply any assumption on the particular boson involved in the non-equilibrium dynamics.

We use the well-known result obtained by Kabanov et al.<sup>10</sup> that, for a d-wave superconductor with a 2D Fermi surface with nodes, the thermal QP population,  $n_T$ , has the form

$$n_T = 1.64N(0)(k_B T)^2/\Delta \quad (2)$$

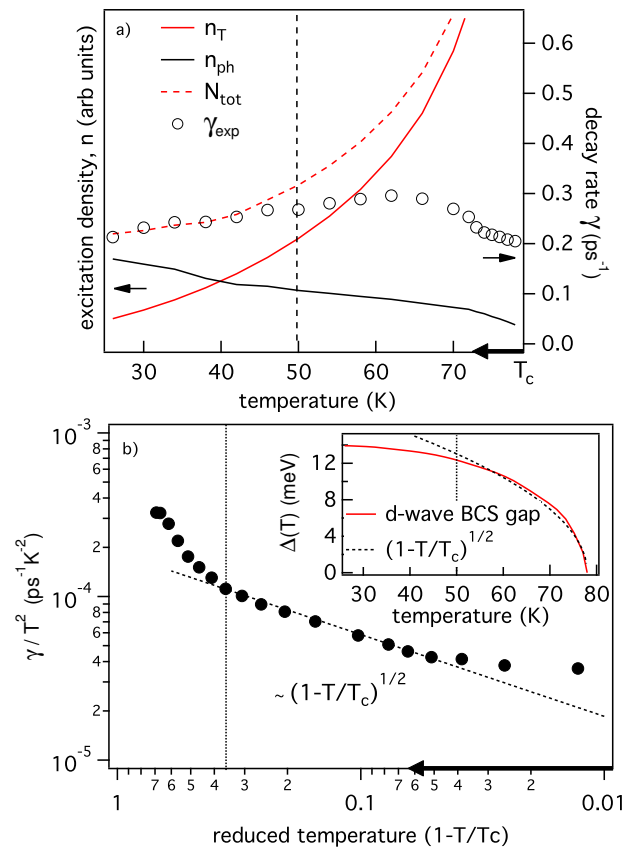


FIG. 2: Panel a) shows the excitation density for both thermal and photoinduced QP, respectively  $n_T$  and  $n_{ph}$  (solid lines), and their sum  $N_{tot}$  (dashed line) as a function of temperature. For the thermal QP we assumed a d-wave like  $\Delta(T)$  dependence (see inset of panel b)). On the right axis we report the experimental decay rate obtained from the fit in Fig. 1. In the b) panel we show  $\gamma/T^2$  as a function of the reduced temperature in a double-logarithmic plot. The long-dashed line represents the  $(1 - T/T_C)^{1/2}$  power-law dependence. In the inset we show the result of the numerical integration of the d-wave BCS gap equation as a function of temperature compared to the  $(1 - T/T_C)^{1/2}$  dependence<sup>33</sup>. In all the panels the vertical short-dashed divide the low from the high temperature regime (see text), above that temperature  $n_T$  is more than double the value of  $n_{ph}$ . In graph b) the error bars are within the black circles size.

where  $N(0)$  is the density of states at the Fermi level and  $\Delta$  is the gap value at equilibrium. The temperature dependence of  $n_T$  obtained from Eq. (2) is plotted in Fig. 2a, together with the  $n_{ph}$  population density obtained from the experimental value of SCS amplitude,  $B$ , assuming their proportionality. In the low-temperature limit,  $\Gamma(T, \Delta)$  shows a weak T-dependence<sup>13</sup> and the experimental decay rate follows the T-dependence of the total quasi-particle density,  $N_{tot} = n_{ph} + n_T$ , as from Eq. (1). Thus we weighted the two contributions,  $n_{ph}$  and  $n_T$ , so that  $N_{tot}$  mimic the slope of the experimental decay rate,  $\gamma_{exp}$  in the low-temperature limit<sup>34</sup>. In the

high-temperature limit we observe that: i) the thermal population  $n_T$  is dominating on  $n_{ph}$ ; ii)  $\gamma_{exp}$  is not following the  $N_{tot}$  temperature dependence. This finding suggests that the decay time increase observed close to  $T_C$  is related to a decrease of  $\Gamma(T, \Delta)$ . We set the separation between the high- and low-temperature regimes at 50 K, i.e., when  $n_T$  is more than double the value of  $n_{ph}$ . However, our conclusions are independent on the particular choice of this temperature.

We now verify that the increase in decay time when approaching  $T_C$  is related to a real divergence arising from the fact that  $\Gamma(T, \Delta) \rightarrow 0$  when  $\Delta \rightarrow 0$  and we find the power-law that controls this divergence. In Fig. 2b, we plot the quantity  $\gamma_{exp}/T^2$  as a function of the reduced temperature (distance from the critical temperature) on a double-logarithmic scale. Using Eqs. (1) and (2), we find that this quantity is proportional to

$$\frac{\gamma}{T^2} \propto \frac{\Gamma(T, \Delta)}{\Delta} \quad (3)$$

in the temperature region where  $n_T$  is the dominant term in the QP density, i.e., above 50 K.

In this region, we notice a power-law dependence with an exponent of 1/2 (solid line in Fig. 2b),

$$\frac{\Gamma(T, \Delta)}{\Delta} \propto (1 - T/T_C)^{1/2} \quad (4)$$

which is the same mean-field critical exponent expected for the order parameter  $\Delta$  in a BCS superconductor. In a d-wave superconductor with  $T_C$  of 78 K, the superconducting gap dependence is well approximated by  $\Delta \propto (1 - T/T_C)^{1/2}$ , in the temperature range from 50 to 78 K (see the inset in Fig. 2b). This assumption is still a good approximation in the case of overdoped HTSC<sup>35-37</sup>. A deviation from this exponent is found a few degrees below  $T_C$ , since Eq. (1) is not applicable in the close vicinity of  $T_C$ <sup>32</sup>.

Thus we can easily derive the power-law dependence of the  $\Gamma(T, \Delta)$  function in the RT approach within the approximate analytic solution (Eq. (1))<sup>32</sup>:

$$\Gamma(T, \Delta) \propto (1 - T/T_C) \propto \Delta^2 \quad (5)$$

This power-law dependence can hardly be derived by first-principles, particularly if the nature of boson involved in the pairing mechanism is unknown.

## B. Discontinuity in the fluence dependence

In Fig. 3a and 3b, we report the  $\Delta R/R$  traces at 10 K obtained at increasing pump intensity. All the curves were fitted using two exponential functions convoluted with the time shape of the laser pulse. The results of the fit are superimposed to the experimental curves. Fig. 3c

shows the SCS amplitude and decay time for each fit as a function of pump fluence. The low-excitation regime, i.e., the regime where the SCS is proportional to the pump fluence is reported in Fig. 3a and in Fig. 3c below 26  $\mu\text{J}/\text{cm}^2$ . In agreement with previous works<sup>3-14,22</sup>, we assume that the SCS is proportional to the photoinduced QP density,  $n_{ph}$ . Thus we conclude that  $n_{ph}$  increases linearly with the pump fluence in this regime.

Above 26  $\mu\text{J}/\text{cm}^2$  the SCS has a sub-linear dependence and we identify this regime as the high-excitation regime<sup>3,8</sup> (Fig. 3b and Fig. 3c above 26  $\mu\text{J}/\text{cm}^2$ ). In this regime, the SCS exhibits a saturation at a critical fluence,  $\Phi_{cr}$ , of  $\sim 55 \mu\text{J}/\text{cm}^2$ . This saturation means that no more Cooper pairs can be destroyed above  $\Phi_{cr}$  and it is evidence of the superconducting condensate vaporization during the laser pump pulse. The fact that the crossover between the linear and the saturated regime is not an abrupt discontinuity here is due to the finite penetration depth of the light pulse<sup>8</sup>. The occurrence of a real phase transition in this regime has been proved by

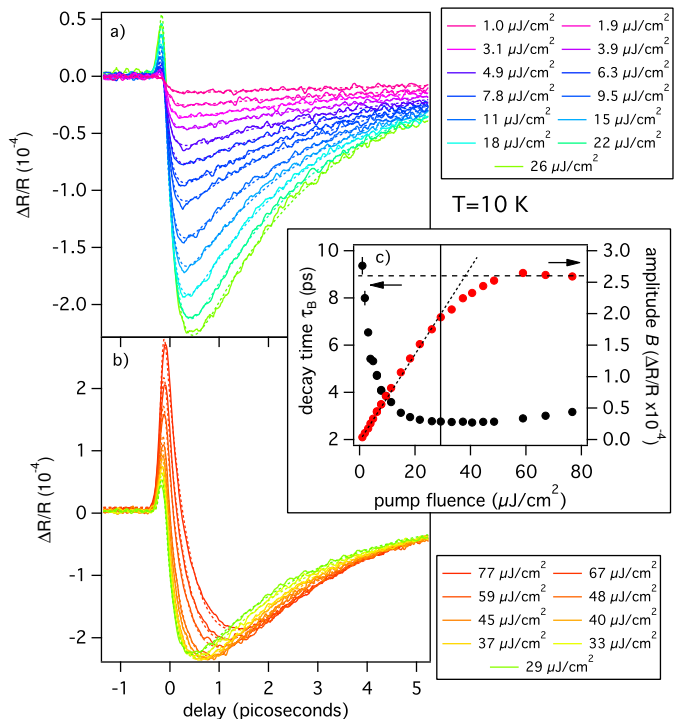


FIG. 3:  $\Delta R/R$  signal, solid lines in panel a) and b), at 10 K as a function of delay time at different pump fluences. The fit to the experimental curves are shown with dashed lines. The fit parameters (decay time  $\tau_B$  and amplitude  $B$ ) are reported in panel c) as a function of pump fluence. In panel a) the low-intensity regime is shown, corresponding to the left hand side of panel c). This regime is characterized by a linear amplitude as a function of fluence (short-dashed line in c)). The panel b) and the right hand side of panel c) correspond to the high-excitation regime, where the SCS amplitude exhibits the saturation already observed in Refs. 3,8,9 (long-dashed line in c)). In panel c) the error bars are within circles size.

measuring the emergence of a fast component above this threshold<sup>3</sup>.

However, the origin of such a non-equilibrium phase transition remains unclear, as it might be the experimental realization of either a first-order non-thermal phase transition, as predicted by the  $\mu^*$  non-equilibrium superconductivity model<sup>1,2</sup>, or a quasi-thermal second order phase transition (T\* model)<sup>2,38</sup>.

To solve this question we report the decay time in the high-excitation regime obtained through a fit to the experimental curves. The decay time is plotted in the right-hand side of Fig. 3c and remains finite in the whole regime, without any tendency to diverge at high fluence.

Comparing the inset of Fig. 1 and Fig. 3c, the difference between the thermal and the photoinduced phase transition is striking. In the former case, the parameter setting the level of perturbation of the system is the sample temperature, while in the latter case this role is played by the pump fluence. Within this analogy the critical fluence,  $\Phi_{cr}$ , at which the SCS exhibits the saturation, is the counterpart of critical temperature,  $T_C$ . If the photoinduced vaporization were a quasi-thermal non-equilibrium phenomenon one would expect a vanishing order parameter at  $\Phi_{cr}$ , as in the thermal case. Thus a diverging decay time would be expected, according to Eq. (5) and Eq. (3). On the contrary, the experimental

results here reported show a decay time that remains finite and below 3.2 ps, thus implying a finite gap at the threshold fluence.

To support this qualitative results with more quantitative arguments, we recall Eq. (1). We recognize the divergence of the decay time in the zero fluence limit (Fig. 3c) as related to the vanishing contribution of  $n_{ph}$  and a very small  $n_T$  term at  $T=10$  K. In facts, plotting the decay rate as a function of pump fluence (Fig. 4a) we see a linear dependence at low fluence, with an intercept of  $0.092 \text{ ps}^{-1}$  related to the finite value of  $n_T$  at  $T=10$  K according to Eq. (1) and Eq. (2). This linear dependence on the pump fluence follows the trend observed on underdoped HTSC<sup>6,12</sup>, but was not observed clearly on overdoped samples<sup>6,39</sup>.

We define a normalized photoinduced decay rate,  $\gamma_{ph}$ ,

$$\gamma_{ph}(T, \Delta(n_{ph}), n_{ph}) \equiv \gamma(T, \Delta(n_{ph}), n_{ph}) - \gamma_T(T, \Delta(0), n_{ph} = 0) \quad (6)$$

that represents the decay rate exclusively due to the photoinduced QPs, where the thermal contribution to the decay rate,  $\gamma_T$ , (intercept in Fig. 4a) has been subtracted. We neglect the sample temperature dependence since in our pump-probe experiment this parameter remains constant. We obtain the formula

$$\gamma_{ph}(\Delta(n_{ph}), n_{ph}) = n_{ph}\Gamma(\Delta(n_{ph})) + n_T[\Gamma(\Delta(n_{ph})) - \Gamma(\Delta(0))] \approx n_{ph}\Gamma(\Delta(n_{ph})) \quad (7)$$

In the right-hand side of Eq. 7 we neglected the second term of the sum. This approximation is valid in the high-excitation regime when  $n_{ph}$  is much larger than  $n_T$ , as long as  $\Gamma$  is not going to zero, which is suggested by the absence of a decay time divergence.

Using Eq. (5)<sup>40</sup> and the proportionality between  $n_{ph}$  and  $\Delta R/R$  we can rewrite Eq. (7) as

$$\gamma_{ph} = \frac{\Delta R}{R} \Delta^2 \quad (8)$$

from which we obtain:

$$\sqrt{\frac{\gamma_{ph}}{\Delta R/R}} \propto \Delta \quad (9)$$

We thus define the quantity  $\delta \equiv \sqrt{\frac{\gamma_{ph}}{\Delta R/R}}$ , proportional to the superconducting gap,  $\Delta$ .

In Fig. 4b we report the value of this quantity, normalized to the zero fluence limit value, obtained from the experimental curves of Fig. 3 as a function of the SCS amplitude. The gap value decreases with  $\Delta R/R$ , hence it decreases with increasing  $n_{ph}$ , as expected<sup>1,2,38</sup>. On the

other side, above the experimental threshold, where  $n_{ph}$  is constant, the non-equilibrium gap remains constant, reflecting the correctness of neglecting the T dependence in  $\Delta(n_{ph}, T)$  and  $\gamma_{ph}(T, \Delta, n_{ph})$ .

We now compare our results with the predictions of the quasi-thermal non-equilibrium superconductivity model, i.e., the T\* model<sup>2,38</sup>, where the non-equilibrium QP population is described by a Fermi-Dirac distribution with an effective temperature T\*. In Fig. 4b we plot the analytical results for  $\Delta(n, T=0)/\Delta(n=0, T=0)$  within this model in the low-excitation limit as a function of the QP density  $n$  for both s-wave and d-wave gap symmetry<sup>2</sup>. The dependence in the d-wave case is  $\propto n^{3/2}$ , while it is linear in the s-wave case. A second-order quasi-thermal phase transition is expected when  $\Delta \rightarrow 0$ .

The main features evidenced by Fig. 4 are: i) a finite value of  $\Delta(n_{max}, T = 10 \text{ K})$  of about 1/2 of the equilibrium value at the fluence threshold, ii) the linear dependence of  $\Delta(n_{ph}, T = 10 \text{ K})$  with  $\Delta R/R$  and thus with  $n_{ph}$ .

The result i) self-consistently confirms our initial assumption of a non-vanishing  $\Gamma$  function, but is in strong contradiction with the predictions of a T\* quasi-thermal



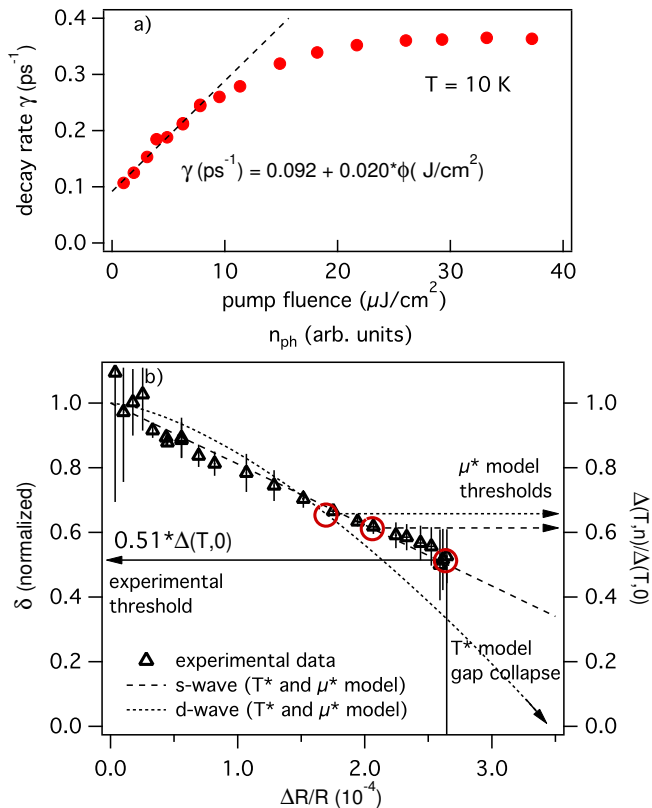


FIG. 4: a) Experimental decay rate extracted by the fit of the  $\Delta R/R$  traces at different pump fluences (see Fig. 3). The dashed line is the linear fit obtained in the low-intensity limit. The error bars are within the circles size. b) We report  $\delta$  as a function of  $\Delta R/R$ . We normalized the value to the zero fluence limit, which correspond to the equilibrium gap  $\Delta(T,0)$ . The error bars indicate the difference between the results obtained starting from the analytic solution of the RT equations (Eq. (1)) and the numerical one (see text). On the same graph (right and upper axis) we show the results the analytical results for the  $\mu^*$  and  $T^*$  model for the superconducting gap,  $\Delta$ , as a function of QP density  $n$  as reported in Ref. 2 for both s-wave and d-wave cases. The threshold values are calculated numerically within the  $\mu^*$  model<sup>2</sup> at a finite temperature corresponding to 10 K in our experiment.

non-equilibrium phase transition. We thus recall the results of the  $\mu^*$  model<sup>1-3</sup>, where the non-equilibrium QP density population is represented by an effective chemical potential  $\mu^*$ , while its temperature remains at the equilibrium value  $T$ . The  $\Delta(n, T = 0)/\Delta(n = 0, T = 0)$  curves show the same power dependence as in the  $T^*$  case<sup>2</sup>. The main difference consists in the prediction of the superconducting-to-normal-state transition, which at 10 K should take place at a relative gap value of  $\approx 60\%$  and  $\approx 65\%$  in the s-wave and d-wave case, respectively<sup>2</sup>. The experimental value obtained in this work is remarkably close to the  $\mu^*$  model predictions, even if a quantitative comparison would require a detailed analysis of the photoinduced QP distribution and an accurate numerical

calculations in the high-fluence regime<sup>2,3</sup>.

The result ii) suggests an s-wave like dependence of the non-equilibrium gap. Even if this finding seems in contradiction with the equilibrium gap d-wave symmetry reported for HTSC<sup>41</sup>, one should bear in mind the fact that the non-equilibrium population photoinduced by a 100 fs laser pulse is uniformly distributed in the  $k$ -space<sup>12</sup>. This leads to a non-thermal effective distribution that can only be reproduced by a Fermi-Dirac statistic with anisotropic effective chemical potential or effective temperature. The result of such anisotropic models are equivalent to those obtained for an s-wave superconductor. An s-wave like gap symmetry was previously used to explain the temperature dependence of  $n_{ph}$  in the low-excitation regime of HTSC<sup>10</sup> and led to a strong controversy in the pump-probe experiments interpretation<sup>2,10</sup>. However, we remark that this result does not imply an s-wave gap symmetry in HTSC at equilibrium and it is rather related to the excitation process.

Both these results suggest a strongly non-thermal QP population behind the observed dynamics. The photoinduced discontinuity observed in several HTSC<sup>3,8,9</sup> can be thus interpreted as the manifestation of a first-order non-thermal phase transition predicted by the  $\mu^*$  model occurring when the gap value has reached about 60% of the equilibrium value.

The results reported in this manuscript are obtained assuming the validity of Eq. (1), which is an approximated analytic solution of the RT equations for  $T < 70$  K<sup>32</sup>. We repeated the same procedure starting from the numerical solution of the RT equations, which is valid in the whole temperature range. However the final results of our work are unaffected. The error bars in Fig. 4b account for the deviation of the analytic results from the numerical one.

#### IV. CONCLUSION

We reported pump-probe experiments on an overdoped Y-Bi2212 sample at 800 nm. We explored both the low- and the high-excitation regimes to clarify the origin of the recently discovered photoinduced vaporization of the superconducting condensate<sup>3,8</sup>. The absence of a signal related to the pseudogap phase in this overdoped sample leads to a clearer interpretation of this phenomenon. We first verified the exponent of the power-law divergence at low-excitation in the vicinity of  $T_C$ . Simply assuming this power-law divergence and no particular bosonic mechanism, we estimated the non-equilibrium order parameter value ( $\Delta$ ) in the high-excitation limit. We found a finite gap value of about 1/2 of the equilibrium gap at the critical fluence at which the photoinduced vaporization occurs ( $\Phi_{cr} \approx 55 \mu\text{J}/\text{cm}^2$ ). This result is a strong indication that the observed photoinduced phase transition has the non-equilibrium 1<sup>st</sup> order character expected in the  $\mu^*$  model<sup>1-3</sup>.

This opens interesting perspectives for the study of

superconductors in general. A non-equilibrium first-order phase transition implies a dynamical competition between coexisting superconducting and normal state phases<sup>3,42</sup>. We expect this dynamics to be experimentally accessible with pump-probe techniques in the femtosecond time domain. The perspective is even more intriguing if one extends this approach to underdoped samples, where the dynamical competition would involve the pseudogap phase as well.

These findings clarify the fundamental interaction of an infrared coherent pulse with the superconducting condensate in HTSC at high excitation pump intensity. This is a landmark for the growing field of pump-probe techniques on HTSC<sup>3,8,9,18–22,43</sup>. Our experiment defines the maximum pump fluence ( $\Phi_{cr} \approx 55 \mu\text{J}/\text{cm}^2$ ) which still allows to probe the superconducting state of Y-Bi2212; it also demonstrates that recent pump-probe experiments performed on Bi2212 at higher pump fluences<sup>18–20</sup> are

dealing with a dynamical competing admixture of superconducting, normal and possibly pseudogap phases.

### Acknowledgments

F.C., G.C., and F.P. acknowledge the support of the Italian Ministry of University and Research under Grant Nos. FIRBRBAP045JF2 and FIRB-RBAP06AWK3. The crystal growth work at Stanford University was supported by DOE under Contracts No. DE-FG03-99ER45773 and No. DE-AC03-76SF00515 and by NSF under Grant No. DMR9985067. The work at UBC was supported by the Killam Program (A.D.), the Alfred P. Sloan Foundation (A.D.), the CRC Program (A.D.), NSERC, CFI, CIFAR Quantum Materials, and BCSI.

- 
- <sup>1</sup> C. Owen and D. Scalapino, Phys. Rev. Lett. **28**, 1559 (1972).
- <sup>2</sup> E. Nicol and J. Carbotte, Phys. Rev. B **67**, 214506 (2003).
- <sup>3</sup> C. Giannetti, G. Coslovich, F. Cilento, G. Ferrini, H. Eisaki, N. Kaneko, M. Greven, and F. Parmigiani, Phys. Rev. B **79**, 224502 (2009).
- <sup>4</sup> P. Gay, D. Smith, C. Stevens, C. Chen, G. Yang, S. Abell, D. Wang, J. Wang, Z. Ren, and J. Ryan, J. Low Temp. Phys. **117**, 1025 (1999).
- <sup>5</sup> P. Gay, C. Stevens, D. Smith, C. Chen, and J. Ryan, Physica C **341**, 2221 (2000).
- <sup>6</sup> N. Gedik, M. Langner, and J. Orenstein, Phys. Rev. Lett. **95**, 117005 (2005).
- <sup>7</sup> G. Coslovich et al., AIP proceedings **1162**, 177 (2009).
- <sup>8</sup> N. Kusan, V. Kabanov, J. Demsar, T. Mertelj, S. Sugai, and D. Mihailovic, Phys. Rev. Lett. **101**, 227001 (2008).
- <sup>9</sup> T. Mertelj, V. Kabanov, C. Gadermaier, N. Zhigadlo, S. Katrych, J. Karpinski, and D. Mihailovic, Phys. Rev. Lett. **102**, 117002 (2009).
- <sup>10</sup> V. Kabanov, J. Demsar, B. Podobnik, and D. Mihailovic, Phys. Rev. B **59**, 1497 (1999).
- <sup>11</sup> D. Dvorsek, V. Kabanov, J. Demsar, S. Kazakov, J. Karpinski, and D. Mihailovic, Phys. Rev. B **66**, 0205100 (2002).
- <sup>12</sup> N. Gedik, P. Blake, R. Spitzer, J. Orenstein, R. Liang, D. Bonn, and W. Hardy, Phys. Rev. B **70**, 014504 (2004).
- <sup>13</sup> V. Kabanov, D. Mihailovic, and J. Demsar, Phys. Rev. Lett. **95**, 147002 (2005).
- <sup>14</sup> R. A. Kaindl, M. A. Carnahan, and D. S. Chemla, Phys. Rev. B **72**, 060510 (2005).
- <sup>15</sup> Y. H. Liu et al., Phys. Rev. Lett. **101**, 137003 (2008).
- <sup>16</sup> P. A. Lee, N. Nagaosa, and X. Wen, Rev. Mod. Phys. **78**, 17 (2006), and references therein.
- <sup>17</sup> J. Demsar, B. Podobnik, V. Kabanov, T. Wolf, and D. Mihailovic, Phys. Rev. Lett. **82**, 4918 (1999).
- <sup>18</sup> R. Saichu, I. Mahns, A. Goos, S. Binder, P. May, S. Singer, B. Schulz, A. Rusydi, J. Unterhinninghofen, D. Manske, et al., Phys. Rev. Lett. **102**, 177004 (2009).
- <sup>19</sup> F. Carbone, D. Yanga, E. Giannini, and A. H. Zewail, Proceedings of the National Academy of Sciences **105**, 20161 (2008).
- <sup>20</sup> L. Perfetti, P. Loukakos, M. Lisowski, U. Bovensiepen, H. Eisaki, and M. Wolf, Phys. Rev. Lett. **99**, 197001 (2007).
- <sup>21</sup> C. Giannetti et al., Phys. Rev. B **80**, 235129 (2009).
- <sup>22</sup> E. E. M. Chia, D. Talbayev, J.-X. Zhu, H. Q. Yuan, T. Park, J. D. Thompson, C. Panagopoulos, G. F. Chen, J. L. Luo, N. L. Wang, et al., Phys. Rev. Lett. **104**, 027003 (2010).
- <sup>23</sup> H. Eisaki, N. Kaneko, D. L. Feng, A. Damascelli, P. K. Mang, K. M. Shen, Z. Shen, and M. Greven, Phys. Rev. B **69**, 064512 (2004).
- <sup>24</sup> High pump fluence measurements were performed at a repetition rate of 108 kHz or less, while low pump fluence ones were obtained at a repetition rate of 540 kHz to maximize the signal-to-noise ratio. The total photon intensity impinging the sample was never higher than 350  $\mu\text{W}$ .
- <sup>25</sup> P. B. Allen, Phys. Rev. Lett. **59**, 1460 (1987).
- <sup>26</sup> S. Brorson et al., Phys. Rev. Lett. **64**, 2172 (1990).
- <sup>27</sup> S. Brorson et al., Solid State Commun. **74**, 1305 (1990).
- <sup>28</sup> M. Tinkham and J. Clarke, Phys. Rev. Lett. **28**, 1366 (1972).
- <sup>29</sup> A. Schmidt and G. Schon, J. Low Temp. Phys. **20**, 207 (1975).
- <sup>30</sup> A. Rothwarf and B. Taylor, Phys. Rev. Lett. **19**, 27 (1967).
- <sup>31</sup> J. Demsar et al., Phys. Rev. Lett. **91**, 267002 (2006).
- <sup>32</sup> Eq. (1) is valid as long as  $n_T \ll N_T$ , where  $N_T$  is the thermal boson population density. The limit  $n_T \sim N_T$  is achieved only in close vicinity of  $T_C$  (see Ref. 13). In Fig. 2a we see that  $n_T$  strongly decreases below  $T_C$ , making the condition  $n_T \ll N_T$  (and thus Eq. (1)) to be valid below 70 K for the sample used in this work.
- <sup>33</sup> M. Tinkham, *Introduction to Superconductivity* (McGraw-Hill, Inc., 1996).
- <sup>34</sup> We remark that the actual values of the quasi-particle densities,  $n_T$  and  $n_{ph}$ , remain unknown. However we properly weighted the relative contributions of  $n_T$  and  $n_{ph}$  to the total quasi-particle density  $N_{tot}$  to mimic the experimental slope as a function of temperature below 50K (Fig. 2a). In particular we considered the first six experimental points

of Fig. 2a.

- <sup>35</sup> W. S. Lee, I. M. Vishik, K. Tanaka, D. H. Lu, T. Sasagawa, N. Nagaosa, T. P. Devereaux, Z. Hussain, and Z. Shen, *Nature* **450**, 81 (2007).
- <sup>36</sup> S. Hufner and F. Muller, *Phys. Rev. B* **78**, 014521 (2008).
- <sup>37</sup> A. Yazdani, *J. Phys.: Condens. Matt.* **21**, 164214 (2009).
- <sup>38</sup> W. Parker, *Phys. Rev. B* **12**, 3667 (1975).
- <sup>39</sup> The slope obtained in this work in the range from 1 to 10  $\mu\text{J}/\text{cm}^2$  is  $0.02 \text{ ps}^{-1}/\mu\text{J}/\text{cm}^2$ , which is compatible, within the experimental uncertainty, with the substantially constant decay rate measured by Gedik et al. in the range from 0.1 to 1  $\mu\text{J}/\text{cm}^2$ .
- <sup>40</sup> As long as Eq. (1) is valid  $n_{ph}$  and  $n_T$  are equivalent and we can apply Eq. (5) obtained in the low-fluence, high-temperature limit to the high-fluence, low-temperature one.
- <sup>41</sup> W. Hardy, D. Bonn, D. Morgan, R. Liang, and K. Zhang, *Phys. Rev. Lett.* **70**, 3999 (1993).
- <sup>42</sup> E. M. Lifshitz and L. P. Pitaevskii, *Physical Kinetics* (Butterworth-Heinemann, Oxford, 1981).
- <sup>43</sup> F. Cilento et al., *Appl. Phys. Lett.* **96**, 021102 (2010).